Efficient Algorithm for Time-Optimal Control of a Two-Link Manipulator

Elke-Barbara Meier*
Ball Aerospace Systems Division, Boulder, Colorado 80306
and
Arthur E. Bryson Jr.†
Stanford University, Stanford, California 94305

A class of optimization problems of interest in the field of robotics is one that seeks to minimize the time required to force a manipulator to travel a specified distance. Robots employ multiple, bounded control inputs. This work describes a new, very fast algorithm for determining minimum-time trajectories for such systems. We have modified the steepest descent method of optimal programming to find time-optimal switch times for bang-bang control systems. The Switch Time Optimization (STO) program has been applied to a two-link manipulator with two control inputs. To find the minimum time for a robot end-effector to travel between two points in its workspace, one must establish the optimal position of the robot with respect to the work station. The algorithm accomplishes this by allowing optimal initial states to be determined along with the time history of the controls. Exact control switch times and optimal initial conditions have been found for minimum-time repositioning maneuvers in which the robot was required to travel a specified distance. The STO algorithm is not limited to use with manipulators; it is applicable to any bang-bang system.

I. Introduction

ROBOTS are currently used for a variety of tasks in industrial applications.[4,11,22] Speeding up their performance could result in obvious commercial benefit. This paper presents a numerical method for determining the time-optimal performance of robots that conduct maneuvers with unconstrained paths.

For path-following tasks, minimum-time control is circumscribed by the requirement that the end-effector must stay on the specified path. Previous investigators[1,15,19] have used the mathematical constraints imposed by this requirement to solve the time-optimal problem for such systems. However, for the category of maneuvers in which the path of the end effector is *free*, the minimum-time problem has proved more difficult, and it is in this area that the work described here represents a contribution.

The computer code we developed (Switch Time Optimization, or STO, algorithm) provides minimum-time control histories and establishes the optimal configuration of the robot with respect to its work space. For example, if one considers a planar, two-link manipulator with revolute joints, and one requires that its tip move between two points as fast as possible, then the STO code computes the open-loop torque time histories of the two motors at the joints and specifies how the robot should be positioned relative to those points. Robot design decisions and workspace layout depend on such information.

The algorithm is fast and accurate, which makes it useful for parametric studies. Relative torque magnitudes, link lengths, or payload mass can be varied, and new optimal trajectories can be found with ease.

Presented as Paper 87-2263 at the AIAA Guidance Navigation and Control Conference, Monterey, CA, Aug. 17-19, 1987; received Sept. 28, 1987; revision received Nov. 17, 1988.

*Senior Member, Technical Staff; currently at The Aerospace Corporation, Los Angeles, CA. Member AIAA.

†Paul Pigott Professor of Engineering, Department of Aeronautics and Astronautics. Fellow AIAA.

Related Work in Robotics

Time-optimal control of robots is a relatively new area of research. Previous investigators who have studied the given endpoint problem for unconstrained paths include Kahn and Roth,[10] Niv and Auslander,[13] Geering et al.,[6] and Sahar and Hollerbach.[17] These researchers all assumed that the optimal controls were bang-bang. Rajan[16] employed the methods of Bobrow et al.[1] to find the time-optimal trajectory for a specified tip path. Rajan then varied the path and did an exhaustive search to find the path with the fastest time-optimal trajectory. Optimal robot placement was not included in any of the studies just cited but was addressed in a restricted way by Scheinman and Roth.[18] All of these methods either involved further limiting assumptions or were computationally prohibitive.

Weinreb[23] and Weinreb and Bryson[24] were the first to obtain substantive information about the minimum-time behavior of the two-link manipulator with open initial conditions. They did not assume that the optimal controls were bang-bang, but results from Weinreb's adjusted control weight (ACW) algorithm, which was based on Bryson's steepest descent algorithm,[3] indicated that most cases tended toward bang-bang. Because the ACW program was a continuous function optimization code, it was unable to achieve sharp discontinuities in the controls, and it was computationally intensive.

The STO algorithm is also based on Bryson's gradient search technique for function optimization but, because it assumes that the trajectories are bang-bang, it not only achieves sharp discontinuities in the controls but also provides large computational savings. The output of the program indicates that the bang-bang assumption is justified and clearly identifies those cases that are singular. Since it is a function optimization code, the STO algorithm constructs all switch time improvements simultaneously, which also gives it an advantage over parameter optimization methods.[5,9]

Mathematical Description and Objectives of Research

The STO algorithm was used to find time-optimal trajectories for a planar two-link manipulator such as the one shown in Fig. 1. The robot consists of two rigid links, each of length L and mass m, with a tip payload of mass M. It is controlled

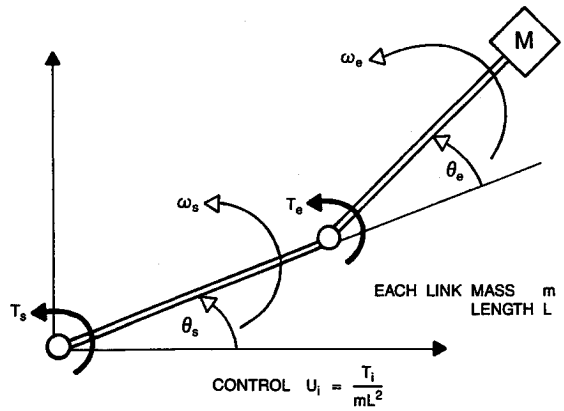

Fig. 1 Two-link manipulator with bounded controls.

by equal bounded torque inputs T_s and T_e at the shoulder and elbow joints, respectively. The controls u_s and u_e are taken to be the corresponding torque divided by mL^2. With proper scaling, the bounds can be set at $+1$ and -1.

The states of the system are the shoulder angle θ_s and the relative (elbow) angle between the two links θ_e, as well as the angular speeds of the links ω_s and ω_e. The dynamic behavior of the system is described by the following state equations, where $\mu = m/M$:

$$\dot{\omega}_s = \frac{1}{\frac{7}{36} + \frac{2}{3}\mu + \left(\mu + \frac{1}{2}\right)^2 \cdot \sin^2\theta_e} \left\{ \left(\mu + \frac{1}{2}\right)^2 \cdot \frac{\sin 2\theta_e}{2} \cdot \omega_s^2 + \left(\mu + \frac{1}{2}\right) \cdot \left(\mu + \frac{1}{3}\right) \cdot \sin\theta_e \cdot \omega_e^2 + \left(\mu + \frac{1}{2}\right) \cdot u_s - \left[\mu + \frac{1}{3} + \left(\mu + \frac{1}{2}\right) \cdot \cos\theta_e\right] \cdot u_e \right\} \tag{1}$$

$$\dot{\omega}_e = \frac{1}{\frac{7}{36} + \frac{2}{3}\mu + \left(\mu + \frac{1}{2}\right)^2 \cdot \sin^2\theta_e} \times \left\{ -\left(\mu + \frac{1}{2}\right) \cdot \left(\mu + \frac{4}{3}\right) \cdot \sin\theta_e \cdot \omega_s^2 - \left(\mu + \frac{1}{2}\right)^2 \cdot \frac{\sin 2\theta_e}{2} \cdot \omega_e^2 - \left(\mu + \frac{1}{2}\right) \cdot \cos\theta_e \cdot u_s + \left[\mu + \frac{4}{3} + \left(\mu + \frac{1}{2}\right) \cdot \cos\theta_e\right] \cdot u_e \right\} \tag{2}$$

$$\dot{\theta}_e = \omega_e - \omega_s \tag{3}$$

$$\dot{\theta}_s = \omega_s \tag{4}$$

The distance the tip is required to travel is

$$D = L\{[1 + \cos\theta_e(t_0) - \cos\theta_s(t_f) - \cos\theta_e(t_f)]^2 + [\sin\theta_e(t_0) - \sin\theta_s(t_f) - \sin\theta_e(t_f)]^2\}^{1/2} \tag{5}$$

Now the minimum-time, given-distance problem for this system may be stated as follows: Find the initial elbow angle (open initial state), final joint angles (open terminal states), and control histories to minimize the time it takes the end-effector to travel a given distance (specified terminal condition), with specified initial and final angular velocities (specified initial and terminal conditions). The optimal quantities are theoretically determined by satisfying Pontryagin's minimum principle.[14]

The system's law of motion is written as a set of n state equations

$$\dot{x} = f(x,u) \tag{6}$$

with $n - k1$ initial conditions

$$x^{(n-k1)}(t_0) = x_0^{(n-k1)} \tag{7}$$

The control u is to be found that transfers the states from x_0^{n-k1} [according to Eq. (6)] to values that satisfy the q ($q \leq n-1$) terminal conditions

$$\Psi(x(t_f), x^{(k1)}(t_0)) = 0 \tag{8}$$

while minimizing the performance index

$$J = \phi(x(t_f), x^{(k1)}(t_0)) = x_n(t_f) = t_f \tag{9}$$

The superscript $(k1)$ on the initial condition vector in Eq. (9) indicates that only $k1$ of the conditions can be varied; the remaining $n - k1$ are specified in Eq. (7). In addition to the n state equations, another system of n equations in the n auxiliary (adjoint) variables $(\Lambda_1, \ldots, \Lambda_n)$ is introduced:

$$\dot{\Lambda}^T = -\Lambda^T f_x \tag{10}$$

We define the Hamiltonian function H, as

$$H(\Lambda, x, u) = \Lambda^T f(x,u) \tag{11}$$

Pontryagin's minimum principle[14] states that, in order for the controls to be optimal, $u(t) = u^*(t)$, resulting in an optimal solution $x(t) = x^*(t)$ to the state equations, 1) the Euler-Lagrange equations must be satisfied:

$$\dot{x} = f(x,u) \tag{12}$$

$$x^{(n-k1)}(t_0) = x_0^{(n-k1)} \tag{13}$$

$$\dot{\Lambda}^T = -\Lambda^T f_x \tag{14}$$

2) the transversality conditions must be met:

$$\Lambda^T(t_f) = \left(\frac{\partial \phi}{\partial x} + \nu^T \frac{\partial \Psi}{\partial x}\right)_{t = t_f} \tag{15}$$

$$(\Lambda^{(k1)})^T(t_0) = -\left(\frac{\partial \phi}{\partial x_0^{(k1)}} + \nu^T \frac{\partial \Psi}{\partial x_0^{(k1)}}\right)_{t = t_f} \tag{16}$$

$$\left(\frac{\partial \phi}{\partial t} + \nu^T \frac{\partial \Psi}{\partial t} + H^*\right)_{t = t_f} = 0 \tag{17}$$

where ν is a $q \times 1$ vector of constant multipliers; 3) the Hamiltonian is minimized:

$$H^*(\Lambda, x^*, u^*) \leq H(\Lambda, x^*, u) \tag{18}$$

and 4) at the terminal time, the Hamiltonian is less than or equal to zero:

$$H^*(t_f) \leq 0 \tag{19}$$

Furthermore, since the minimum Hamiltonian H^* is not explicitly a function of time, H^* is constant and, in view of Eq. (17),

$$H^*(\Lambda(t),x^*(t),u^*(t))=0 \tag{20}$$

When the bounded controls appear linearly in the Hamiltonian, as they do in this case, Pontryagin's principle leads to the result[2] that the controls will be saturated (bang-bang) according to

$$u_i(t)=\begin{cases}+1 & \text{if } H_{u_i}<0\\ -1 & \text{if } H_{u_i}>0\end{cases} \tag{21}$$

Here it was again assumed that the control bounds are unity. The quantity H_{u_i} is called the switching function for u_i.

There is one other possibility. Singular arcs may occur during which the switching function for a control may be identically zero for a finite interval of time, $H_{u_i}=0$, in which case Eq. (21) does not establish the optimal control, which may be between the bounds. However, the results obtained by assuming the controls of the robot are bang-bang are extremely close to optimal even during singular arcs.

The STO algorithm constructs a solution to this problem in the manner of gradient techniques by integrating the state equations forward in time using an initial guess of the unknown quantities $\boldsymbol{u}$, $\boldsymbol{x}_0^{(k1)}$, and t_f. The nominal final states are found and, following backward integration of the adjoint equations, the optimality and terminal conditions are checked. If they are not satisfied, improvements in the initial states, final time, and control histories are formulated and added to the nominal values. However, because our program assumes that the controls are bang-bang, the initial control guesses only involve the switch times, as do the control improvements. How the improvements are formulated is discussed next.

II. Derivation of the Algorithm

The STO algorithm determines the m bang-bang controls $\boldsymbol{u}(t)$, the $k1$ initial conditions $\boldsymbol{x}_0^{(k1)}$, and t_f that minimize the cost functional (9) and meet the terminal conditions (8). The approach taken closely follows that of the first-order gradient method of Bryson and Ho.[2] The details of all the steps taken here are fully explained in the dissertation of Meier.[12] The dynamic constraints (6) are adjoined[7,2] to the cost (9) with a vector of Lagrange multipliers $\boldsymbol{\lambda}$ to create the augmented performance index J^0,

$$J^0=\phi(\boldsymbol{x}(t_f),\boldsymbol{x}^{(k1)}(t_0))+\int_{t_0}^{tf}\boldsymbol{\lambda}^T(\boldsymbol{f}-\dot{\boldsymbol{x}})\,\mathrm{d}t \tag{22}$$

Then the trajectory must be found such that the variations in J^0 and Ψ with respect to $\boldsymbol{u}$, $\boldsymbol{x}_0^{(k1)}$, and t_f vanish. In other words, improvements $\delta\boldsymbol{u}$, $\delta\boldsymbol{x}_0^{(k1)}$, and $\mathrm{d}t_f$ will be determined so as to drive $\mathrm{d}J^0$ and $\mathrm{d}\Psi$ to zero.

$$\mathrm{d}J^0=\left[\left(\frac{\partial\phi}{\partial\boldsymbol{x}_0^{(k1)}}\right)_{t=t_f}+(\boldsymbol{\lambda}^{(k1)})^T_{t=t_0}\right]\delta\boldsymbol{x}_0^{(k1)}+\left(\frac{\partial\phi}{\partial t}+\boldsymbol{\lambda}^T\dot{\boldsymbol{x}}\right)_{t=t_f}\mathrm{d}t_f+\int_{t_0}^{tf}\boldsymbol{\lambda}^T\frac{\partial\boldsymbol{f}}{\partial\boldsymbol{u}}\delta\boldsymbol{u}\,\mathrm{d}t \tag{23}$$

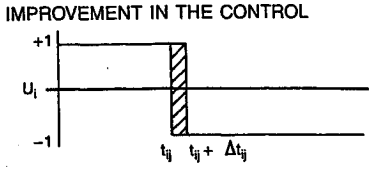

Fig. 2 Control history changes in the STO algorithm.

$$\mathrm{d}\Psi=\left[\left(\frac{\partial\Psi}{\partial\boldsymbol{x}_0^{(k1)}}\right)_{t=t_f}+(\boldsymbol{R}^{(k1)})^T_{t=t_0}\right]\delta\boldsymbol{x}_0^{(k1)}+\left(\frac{\partial\Psi}{\partial t}+\boldsymbol{R}^T\dot{\boldsymbol{x}}\right)_{t=t_f}\mathrm{d}t_f+\int_{t_0}^{tf}\boldsymbol{R}^T\frac{\partial\boldsymbol{f}}{\partial\boldsymbol{u}}\delta\boldsymbol{u}\,\mathrm{d}t \tag{24}$$

Here $\boldsymbol{R}$ is a $(n\times q)$ matrix of Lagrange multipliers, which may be added to $\boldsymbol{\lambda}$ using q constant multipliers $\boldsymbol{\nu}$ to obtain the system adjoint variables $\boldsymbol{\Lambda}$, $(\boldsymbol{\Lambda}=\boldsymbol{\lambda}+\boldsymbol{R}\boldsymbol{\nu})$. The differential of the terminal conditions (24) may be adjoined to the corresponding differential of the performance index (23) via the multipliers $\boldsymbol{\nu}$:

$$\mathrm{d}J^1=\left[\left(\frac{\partial\phi}{\partial\boldsymbol{x}_0^{(k1)}}+\boldsymbol{\nu}^T\frac{\partial\Psi}{\partial\boldsymbol{x}_0^{(k1)}}\right)_{t=t_f}+(\boldsymbol{\Lambda}^{(k1)})^T_{t=t_0}\right]\delta\boldsymbol{x}_0^{(k1)}+\left(\frac{\partial\phi}{\partial t}+\boldsymbol{\nu}^T\frac{\partial\Psi}{\partial t}+\boldsymbol{\Lambda}^T\dot{\boldsymbol{x}}\right)_{t=t_f}\mathrm{d}t_f+\int_{t_0}^{tf}\frac{\partial H}{\partial\boldsymbol{u}}\delta\boldsymbol{u}\,\mathrm{d}t \tag{25}$$

The derivation of Meier[12] extends that of Bryson and Ho[2] to include the variations in the $(n-k1)$ initial conditions. Looking at $\mathrm{d}J^1$, one can identify clearly the gradients with respect to the quantities to be optimized, and $\delta\boldsymbol{x}_0^{(k1)}$, $\mathrm{d}t_f$, and $\delta\boldsymbol{u}$ must be chosen to drive those gradients to zero.

The STO algorithm differs from other function optimization schemes in that it does not calculate impulsive improvements in the controls $\delta\boldsymbol{u}$ at each integration time step. Rather, it assumes that the controls are always saturated (the nominal control history is bang-bang) and calculates variations in the controls only near the switch times. Hales[8] used a similar approach to solve minimum-fuel problems. Figure 2 shows that the control variations are constrained in magnitude to equal the difference in the control limits. The variation in the ith control component u_i is then equal to zero everywhere except at the $st(i)$ nominal switch times. At those times, t_{ij} $(i=1,\ldots,m,\ j=1,\ldots,st(i))$, the variation equals $\Delta u_i=2$ for some short period of time $\mathrm{d}t_{ij}$.

$$\delta u_i=\begin{cases}\Delta u_i & \text{for } t_{ij}\le t<t_{ij}+\mathrm{d}t_{ij}\\ 0 & \text{for all other } t\end{cases} \tag{26}$$

The critical quantities to determine, then, are the changes $\mathrm{d}t_{ij}$ in the nominal switch times. *Note that all the variations in all of the controls are calculated simultaneously at each iteration.*

With the control variation limited as in Eq. (26), the integral in Eq. (25) may be replaced by a summation over the switch time variations:

$$\mathrm{d}J^1=\left[\left(\frac{\partial\phi}{\partial\boldsymbol{x}_0^{(k1)}}+\boldsymbol{\nu}^T\frac{\partial\Psi}{\partial\boldsymbol{x}_0^{(k1)}}\right)_{t=t_f}+(\boldsymbol{\Lambda}^{(k1)})^T_{t=t_0}\right]\delta\boldsymbol{x}_0^{(k1)}+\left(\frac{\partial\phi}{\partial t}+\boldsymbol{\nu}^T\frac{\partial\Psi}{\partial t}+\boldsymbol{\Lambda}^T\dot{\boldsymbol{x}}\right)_{t=t_f}\mathrm{d}t_f+\sum_{i=1}^{m}\sum_{j=1}^{st(i)}\left(\frac{\partial H}{\partial u_i}\right)_{t=t_{ij}}\Delta u_i\,\mathrm{d}t_{ij} \tag{27}$$

Now all that is left to do is find the improvements $\delta\boldsymbol{x}_0^{(k1)}$, $\mathrm{d}t_f$, and $\mathrm{d}t_{ij}$ to make $\mathrm{d}J^1$ vanish. It may be shown[12] that the following choices accomplish this:

$$\delta\boldsymbol{x}_0^{(k1)}=-\boldsymbol{V}^{-1}\left[\left(\frac{\partial\phi}{\partial\boldsymbol{x}_0^{(k1)}}+\boldsymbol{\nu}^T\frac{\partial\Psi}{\partial\boldsymbol{x}_0^{(k1)}}\right)_{t=t_f}+(\boldsymbol{\Lambda})^T_{t=t_0}\right]^T \tag{28}$$

$$\mathrm{d}t_f=-\frac{1}{b}\left(\frac{\partial\phi}{\partial t}+\boldsymbol{\nu}^T\frac{\partial\Psi}{\partial t}+\boldsymbol{\Lambda}^T\dot{\boldsymbol{x}}\right)_{t=t_f} \tag{29}$$

$$dt_{ij} = -\frac{W_{ii}^{-1}}{\Delta u_i}\left(\frac{\partial H}{\partial u_i}\right)_{t=t_{ij}} \tag{30}$$

Here W_{ii} are the elements of a diagonal ($m \times m$) positive-definite weighting matrix W, V is a $k1 \times k1$ positive-definite weighting matrix, and b is a positive constant.

Equations (28-30) are the changes found at each iteration to improve the performance index and reduce errors in the terminal conditions. The STO algorithm solves for the quantities ν by using the calculated value of the terminal conditions and Eqs. (28-30) in an expression for $d\Psi$ similar to Eq. (24) but with the integral replaced by a summation over dt_{ij}. The mathematics and the significance of this step may be found in Meier,[12] along with suggestions for choosing appropriate weighting matrices. When the program has converged, Pontryagin's conditions for optimality are satisfied.

Upon convergence, the STO algorithm furnishes locally optimal solutions to the bang-bang minimum-time problem as long as H_{u_i} is not identically zero over a finite period of time. We will show later that the program produces locally optimal trajectories in most cases. In those few cases in which optimality cannot be determined ($H_{u_i} = 0$ over a finite interval), it will be argued that the results for a two-link manipulator are at least very near optimum. In addition, an argument will be made that the results are globally optimal.

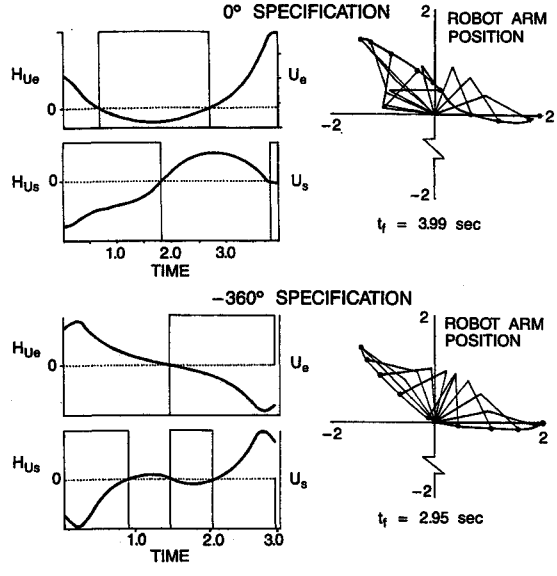

Fig. 3 Comparison of trajectories for different $\theta_e(t_f)$.

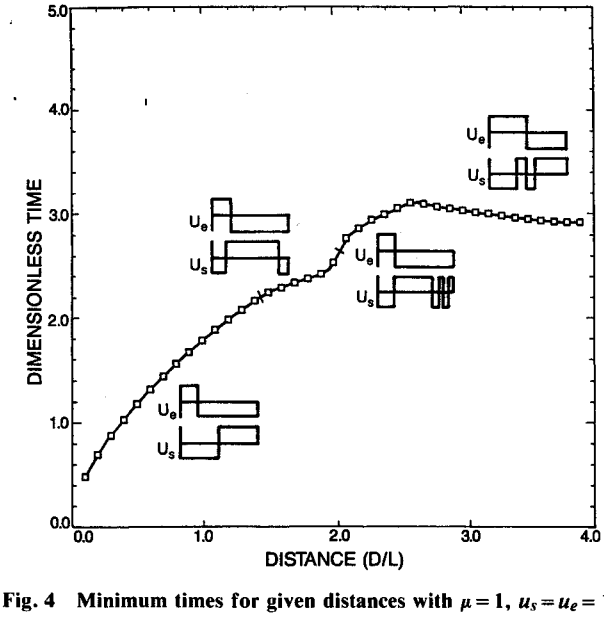

Fig. 4 Minimum times for given distances with $\mu = 1$, $u_s = u_e = 1$.

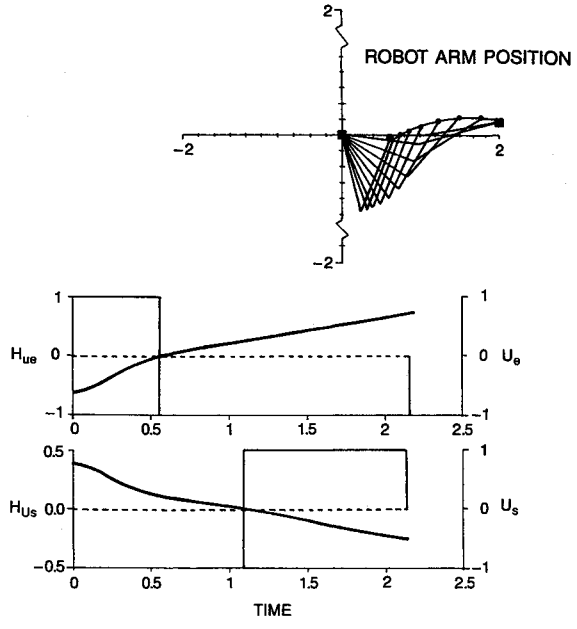

Fig. 5 Trajectory and controls for $D/L = 1.4$; $t_{s1} = 1.08$, $t_{e1} = 0.56$, $t_f = 2.16$, $\theta_{e0} = 0.16$ rad.

Obtaining Good Initial Guesses

To get started, the STO code requires an initial guess of the switch times. The most important measure for choosing the starting conditions is whether the choice will converge to a globally optimal solution. There are a number of ways in which a given distance may be achieved, and many local minima are possible. The Seed algorithm,[12] which solves an approximation to the problem of interest, was written to provide good initial guesses for the STO program. It does not assume that the controls are bang-bang, but it approximates the bounds on the controls by adding to the cost function terms that penalize the deviation of the controls away from the bounds.

$$J = \int_{t_0}^{t_f} [1 + B(u_e^2 - 1)^2 + B(u_s^2 - 1)^2]\, dt \tag{31}$$

For this problem, the Hamiltonian is nonlinear in the controls

$$H = 1 + B(u_e^2 - 1)^2 + B(u_s^2 - 1)^2 + \Lambda^T f \tag{32}$$

and non-bang-bang, nonsingular solutions may be found by employing an extension of Bryson's FCNOPT[3] algorithm for continuous function optimization. The weighting B on the deviation from $\|u_i\| = 1$ was chosen to be 100 by trial and error to produce the best combination of minimum-time and minimum control excursion.

The Seed program is easy to use, as one can start with an initial guess of zero for both controls. The gradient procedure then drives the controls toward their bounds to minimize the performance index. The times at which the controls cross zero are used as initial guesses for the t_{ij} in the STO program. The code gives a good indication of not only how many switches there are but also where they might occur.

The Seed program was used to make a number of runs with various fixed initial and terminal conditions. It showed what form of control histories are required for different types of maneuvers and which types of trajectories are fastest. A good example of the kind of information gained from the Seed program is shown in Fig. 3. The plots and figures are from the STO program, but the initial guesses came from the Seed

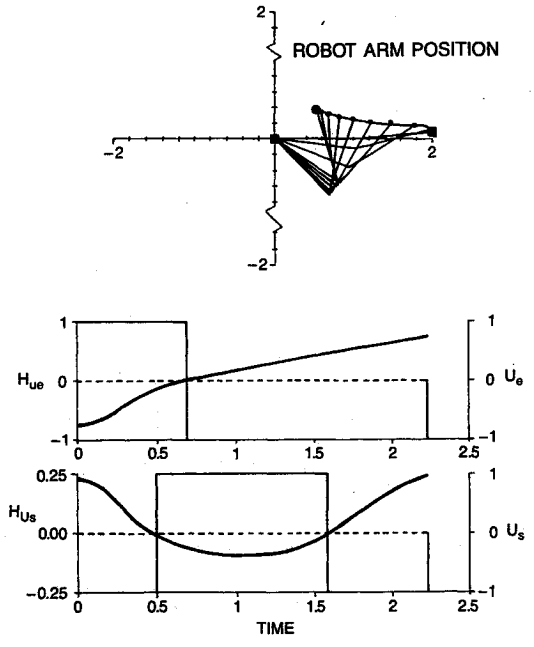

Fig. 6 Optimal trajectory and controls for $D/L = 1.5$; $t_{s1,2} = 0.47$, 1.59; $t_{e1} = 0.68$; $t_f = 2.24$; $\theta_{e0} = 0.08$ rad.

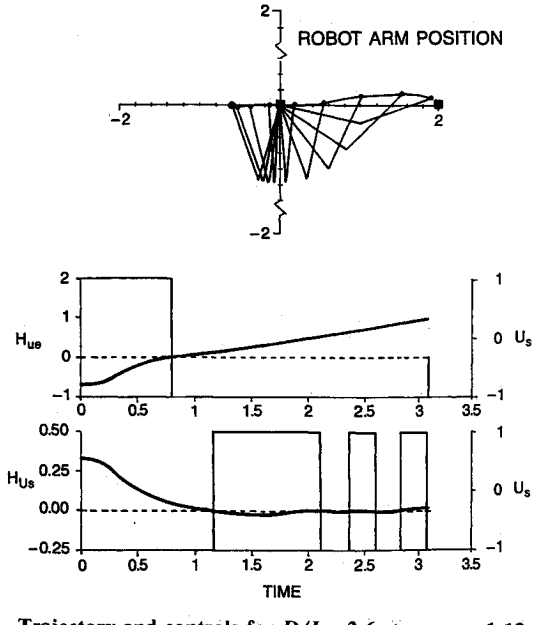

Fig. 7 Trajectory and controls for $D/L = 2.6$; $t_{s1,2,3,4,5} = 1.13$, 2.12, 2.32, 2.60, 2.81; $t_{e1} = 0.81$; $t_f = 3.10$; $\theta_{e0} = 0.03$ rad.

algorithm. A given distance can be achieved in a number of ways, even when the endpoints of the tip are specified. In this case, the endpoints are

$$(x_0,y_0) = (0.0,0.0), \qquad (x_f,y_f) = (-0.707,0.707) \tag{33}$$

and the distance (normalized to link length) is

$$D/L = 3.6955 \tag{34}$$

However, the terminal states in terms of joint angles can be defined in an infinite number of ways. We will examine two of them. First, let the end states be specified as

$$\theta_s(t_0) = 0.0 \text{ deg}, \qquad \theta_e(t_0) = 0.0 \text{ deg}$$

$$\theta_s(t_f) = 135.0 \text{ deg}, \qquad \theta_e(t_f) = 0.0 \text{ deg} \tag{35}$$

At the top right of Fig. 3, the arm is shown at 11 consecutive instances in time, and the curved line is the path the tip follows. The controls that produce this trajectory and the corresponding H_{u_i} are plotted to the left. The total time it takes to perform this maneuver is 3.99 s.

Now let us specify the boundary conditions as

$$\theta_s(t_0) = 0.0 \text{ deg}, \qquad \theta_e(t_0) = 0.0 \text{ deg}$$

$$\theta_s(t_f) = 135.0 \text{ deg}, \qquad \theta_e(t_f) = -360.0 \text{ deg} \tag{36}$$

The results are depicted in the lower half of Fig. 3. The new trajectory looks quite different and is symmetric with respect to the hub (shoulder). The controls are symmetric about $t_f/2$ and display one switch in the elbow and three in the shoulder. The final time for this maneuver is 2.95 s, which represents a 26% improvement over the previous trajectory. Obviously, input control histories similar to the second set are better initial guesses for large distances.

III. Results

The STO program was used to find minimum-time trajectories of the two-link manipulator for given distances D traveled by the tip, ranging from $D/L = 0.0$ to the maximum possible distance $D/L = 4.0$. For the first set of results, the tip mass of the manipulator was set equal to the mass of a link, so that $\mu = 1$, and both control input limits ($\|u_s\|_{\max}$ and $\|u_e\|_{\max}$) were set at $+1$ and -1. Runs were made with these parameters for the full range of distances in steps of $D/L = 0.1$. The results fell into four distinct categories, which depended on the distance traveled. In Fig. 4, minimum final times are plotted against distance traveled. The distance is measured in terms of link lengths, and the time is measured in units of $1/\sqrt{T_{\max}/mL^2}$.

The sketches of control histories next to the curve are representative of the *shape* of the controls in the four sections of the plot. For distances from 0 to 1.4, each control has one switch, with the elbow torque switching at about $t_f/3$ and the shoulder torque at $t_f/2$. For distances from 1.5 to 2.0, the elbow switch is about the same as before, but the shoulder now has two switches. The third group of trajectories, from $D/L = 2.1$ to 2.6, is the one that contains singular arcs. The many switches in the shoulder control toward the end of the maneuver indicate the region of the singularity. The last category contains

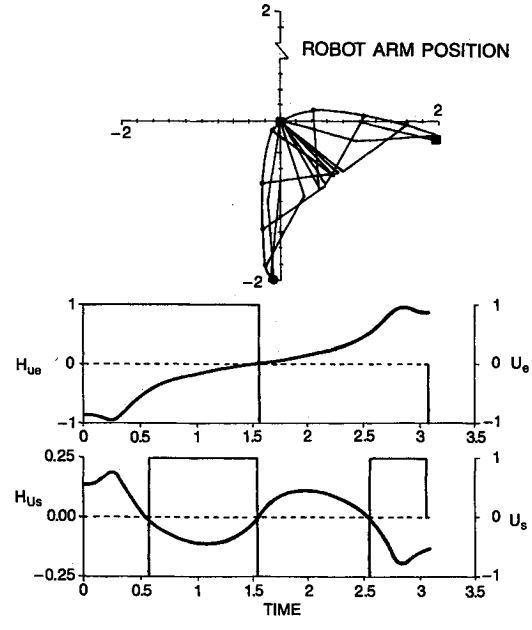

Fig. 8 Optimal trajectory for $D/L = 2.7$; $t_{s1,2,3} = 0.54$, 1.54, 2.54; $t_{e1} = 1.55$; $t_f = 3.09$; $\theta_{e0} = -0.24$ rad.

trajectories that are symmetric. Notice that, at these large distances, the final times actually *decrease.*

$D/L = 0.0$ to 1.4

Figure 5 depicts the minimum-time trajectory and control histories for $D = 1.4$. It is typical of short-distance maneuvers. The arm is shown in consecutive positions during the maneuver. The curved line is the path the tip follows. The controls are again shown with the corresponding gradients of the Hamiltonian superimposed to emphasize the gradient nature of the algorithm and to show the optimality of the solution.

$D/L = 1.5$ to 2.0

At $D/L = 1.5$, the control histories differ considerably from those at $D/L = 1.4$. Figure 6 shows that there are now two switches in the shoulder control, and the tip path has also changed shape somewhat. The manipulator begins from an extended position to get maximum efficiency from the torques. As the arm folds up, the controls are not as effective, and the shoulder has to change sign to "wait" for the elbow torque to bring the tip to a stop. The nature of the trajectories remains unchanged to a distance of 2.0.

Singular Regions

The trajectories from $D/L = 2.1$ to 2.6 contain singular arcs in the shoulder control. Figure 7 depicts a typical case with a singular arc. The STO code maintains bang-bang controls at all times and handles regions in which H_{u_i} is close to zero by putting in a large number of switches. Some of those switches may coalesce during the gradient process. Experience indicates that it makes little difference how many switches are in the singular regions; there is only about a 1% change in t_f for different numbers of switches. Hence, although the optimal control history cannot be found with the STO code, the bang-bang approximations that are obtained are very close to optimal. The Hamiltonian found for these cases was very close to zero [Eq. (20)], which lends further support to this contention. The observation that the singular arcs only occur in one control is in keeping with Sontag and Sussmann's[20,21] contention that if one control is singular, the other cannot be singular.

Symmetric Trajectories

The last category of trajectories is perhaps the most interesting because the final times decrease with increasing distance.

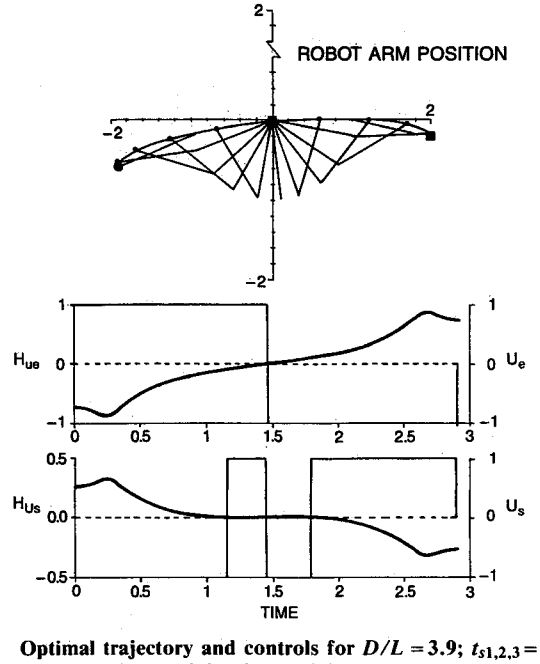

Fig. 9 Optimal trajectory and controls for $D/L = 3.9$; $t_{s1,2,3} = 1.13$, 1.44, 1.77; $t_{e1} = 1.46$; $t_f = 2.91$; $\theta_{e0} = -0.21$ rad.

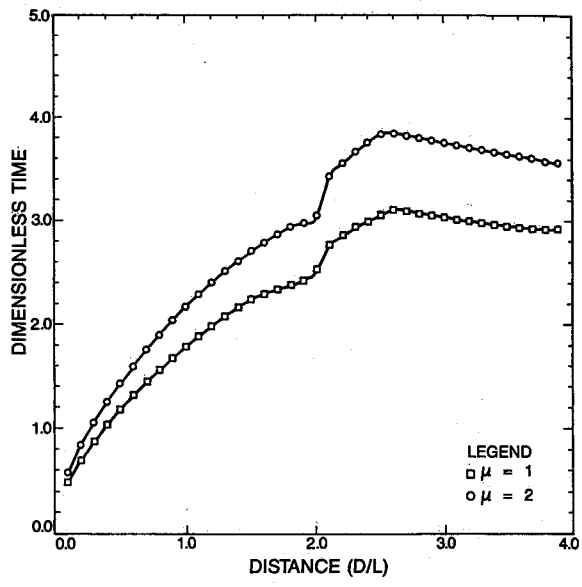

Fig. 10 Comparison of final times for different tip masses.

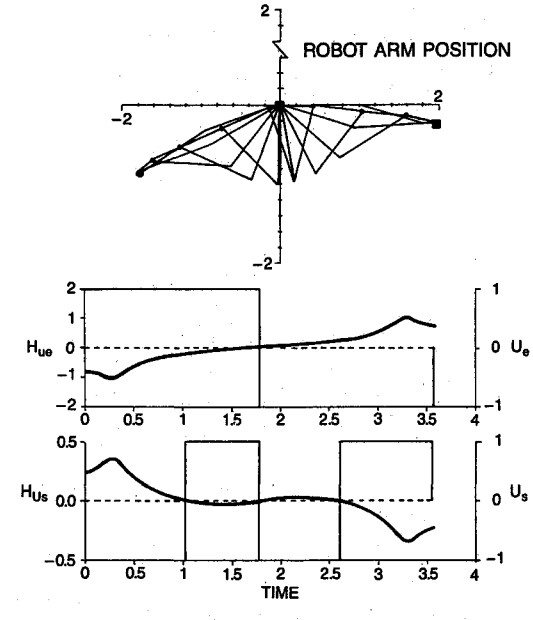

Fig. 11 Suboptimal trajectory for $\mu = 2$ and $D/L = 3.8$; $t_{s1,2,3} = 0.98$, 1.79, 2.59; $t_{e1} = 1.79$; $t_f = 3.58$; $\theta_{e0} = -0.27$ rad.

In Fig. 8, the shortest symmetric minimum-time trajectory is shown. With $D/L = 2.7$, the final time is 3.09. Figure 9 shows a typical long-distance maneuver. Now the final time has decreased to 2.91 for a distance of 3.9. Note that the three switches in u_s have moved closer together. Because the controls are most effective when they are of opposite sign, they are "helping" each other for most of this trajectory. For the shorter distance in Fig. 8, the upper arm is not allowed to travel as far; hence, it must slow itself down in the middle of the trajectory while the elbow swings around more than 360 deg. To accomplish this, the middle switches spread themselves out, causing the controls to be of opposite sign less of the time. In the long-distance maneuver, H_{u_s} approaches zero again near the middle of the trajectory. The STO algorithm has no difficulty in finding the correct switches despite the small gradient. Only for $D/L > 3.99$ and larger tip mass ($\mu = 2$) do difficulties arise. This will be discussed in the next subsection.

The shorter-distance symmetric trajectories are quite sensitive. The minima seem to be very narrow; they are not easy to

find because broader local minima exist in which each control has one switch.

Effects of Increasing the Tip Mass

Figure 10 compares the minimum final times for given distances for $\mu = 1$ and $\mu = 2$. The shapes of the curves are quite similar, and the various regions of similar trajectories are comparable. The final times for the larger payload are about 20% higher than those for $\mu = 1$. Although the general shape of the torque histories is the same for both $\mu = 1$ and $\mu = 2$, the robot trajectory for the larger tip mass differs for large D/L. A trajectory similar to the one for $\mu = 1$ is shown in Fig. 11. Even at the very large distance of 3.8, the three shoulder switches are quite spread out. This means that the controls are not very efficient in the middle part of the trajectory. Another type of trajectory for the same distance, which results in a slightly smaller final time, $t_f = 3.57$, is shown in Fig. 12. Here the shoulder control switches are much closer

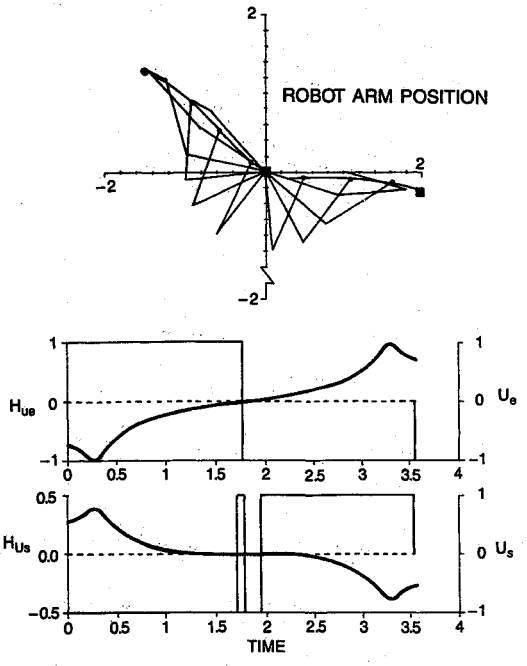

Fig. 12 Optimal trajectory for $\mu = 2$ and $D/L = 3.8$; $t_{s1,2,3} = 1.64$, 1.78, 1.92; $t_{e1} = 1.78$; $t_f = 3.57$; $\theta_{e0} = -0.25$ rad.

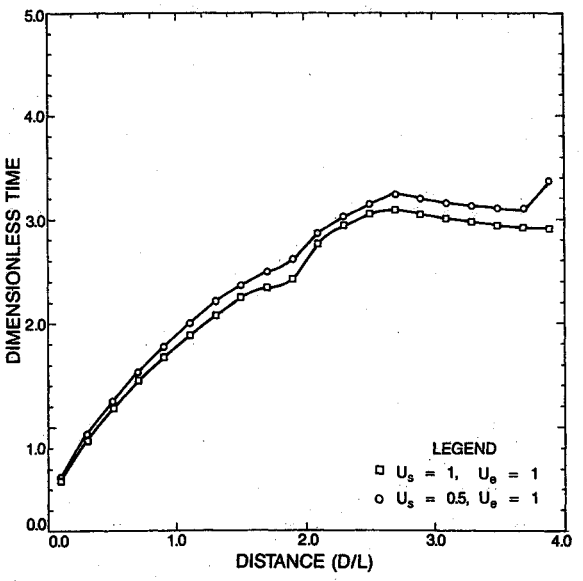

Fig. 13 Final times vs given distances for $\|u_s\| = 0.5$ compared to $\|u_s\| = 1.0$.

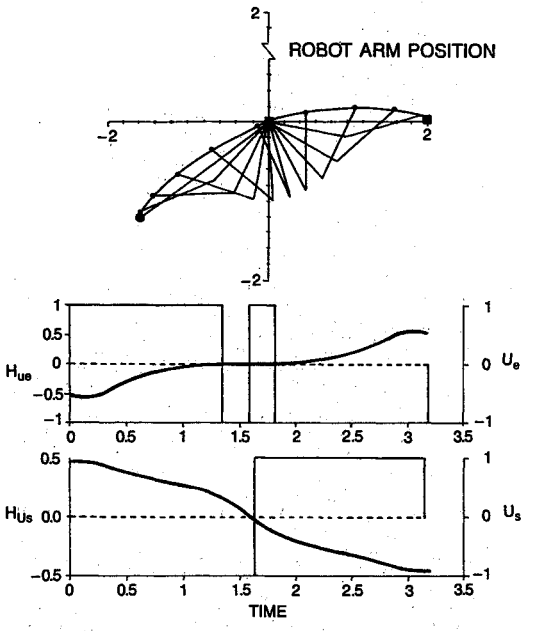

Fig. 14 Trajectory and controls for $D/L = 3.8$ with $\|u_s\| = 0.5$; $t_{s1} = 1.59$; $t_{e1,2,3} = 1.35$, 1.57, 1.82; $t_f = 3.18$; $\theta_{e0} = 0.03$ rad.

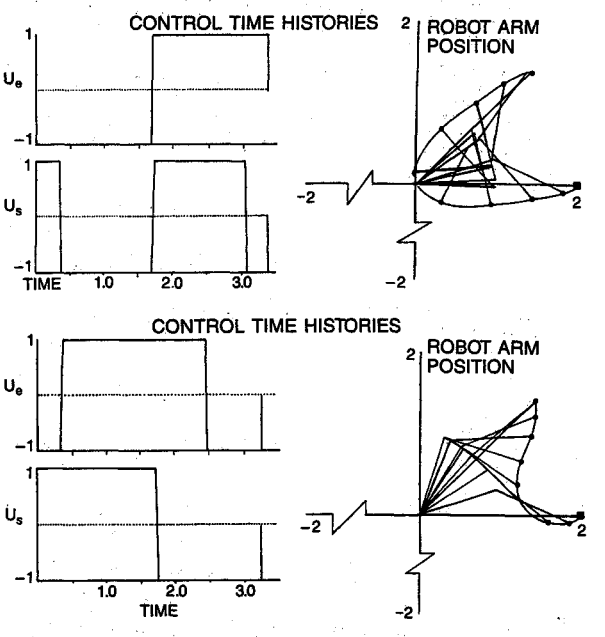

Fig. 15 Comparison of time-optimal and "conventional" trajectories. Optimal: $t_{s1,2,3} = 0.35$, 1.70, 3.04; $t_{e1} = 1.69$; $t_f = 3.40$. Conventional: $t_{s1} = 1.73$; $t_{e1,2} = 0.35$, 2.44; $t_f = 3.45$.

together, and the shoulder travels quite a bit farther than in Fig. 11. For distances less than or equal to 3.7, the "shorter" trajectory is optimal and, for distances greater than 3.8, the "longer" trajectory with the closely spaced shoulder switches is optimal. This implies that there must be a "transition" distance very near 3.8, for which both types of trajectories have the same final time. Consequently, the minimum-time, given-distance trajectories for the two-link manipulator are not unique in all cases. The slight increase in the final time at distances near 4.0 may be explained by the fact that the boundary between the two types of trajectories (as in Figs. 11 and 12) becomes obscured as the maneuver, by necessity, approaches the slower type of trajectory.

Effects of Decreasing the Shoulder Control

Another set of runs was made to investigate the occurrence of singular arcs. Since it was always the shoulder motor that

needed to "slow down and wait" for the elbow to complete its maneuver, we thought it might be informative to decrease the relative magnitude of the shoulder torque with respect to the elbow torque. Figure 13 depicts the results of setting the shoulder control limits at $+0.5$ and -0.5. Compared to the original curve for $\|u_s\| = \|u_e\| = 1.0$ with $\mu = 1$, not only does the final time vs specified distance plot for $\|u_s\| = 0.5$ with $\mu = 1$ look similar and contain comparable trajectory categories, but the final times are increased by only about 5%! Given that cutting *both* controls in half would increase the final times by 41% (i.e., a factor of $\sqrt{2}$), this is somewhat surprising. No evidence was found that halving the shoulder control affects the singular arcs. However, as can be seen from the chart, the final times increase considerably above $D/L = 3.8$ because, with the weaker shoulder control, the elbow control has to wait for the upper arm to "catch up" at large distances. In Fig. 14, one can see that the elbow exhibits an extra pair of switches in the middle of the trajectory to help slow down the lower arm while the shoulder moves through the required distance.

IV. Summary

The STO algorithm, a new numerical method for finding switch times for minimum-time bang-bang systems, has been presented. It is significantly faster than previous approaches to the problem (as much as 100 times faster than the ACW algorithm[23]) and handles multi-input systems.

The Seed program was introduced for obtaining good initial guesses for the STO program and for gaining preliminary insight into the behavior of the time-optimal system.

The combination of the Seed program and the STO code was used to find time-optimal trajectories of the two-link robot for many different specified distances. It was found that time-optimal trajectories can provide around 30% time savings over more conventional trajectories. Figure 15 illustrates that it may be desirable to build a robot with joints that have more than 360-deg relative rotation.

The speed of the STO algorithm allowed us to make a large number of runs and study a wide variety of cases. As a result, we found several different categories of optimal trajectories, including singular cases, and are fairly certain that the results are globally optimal.

Acknowledgment

This work was supported in part by Air Force Office of Scientific Research Contract 82-0062.

References

[1]Bobrow, T. E., Dubowsky, S., and Gibson, J. S., "On the Optimal Control of Robotic Manipulators with Actuator Constraints," *Proceedings of the American Control Conference,* San Francisco, June 1983, pp. 782–789.

[2]Bryson, A. E., Jr., and Ho, Y-C., *Applied Optimal Control—Optimization, Estimation, and Control,* Hemisphere, Washington, DC, 1975.

[3]Bryson, A. E., Jr., *FCNOPT Computer Program,* Department of Aeronautics and Astronautics, Stanford Univ., Stanford, CA, 1982.

[4]Craig, J. J., *Introduction to Robotics,* Addison-Wesley, Reading, MA, 1986.

[5]Davison, E. J., and Monro, D. M., "A Computational Technique for Finding Time Optimal Controls of Nonlinear Time-Varying Systems," *Joint Automatic Control Conference of the American Automatic Control Council,* Boulder, CO, Aug. 1969, pp. 270–282.

[6]Geering, H. P., Guzzella, L., Hepner, S. A. R., and Onder, C. H., "Time-Optimal Motions of Robots in Assembly Tasks," *Proceedings of 24th Conference on Decision and Control,* Ft. Lauderdale, FL, Dec. 1985.

[7]Gelfand, I. M., and Fomin, S. V., *Calculus of Variations,* Prentice-Hall, Englewood Cliffs, NJ, 1963.

[8]Hales, K. A., *Minimum-Fuel Attitude Control of a Rigid Body in Orbit by an Extended Method of Steepest Descent,* Ph.D. Dissertation, Div. of Engineering Mechanics, Stanford Univ., Stanford, CA, March 1966.

[9]Jacoby, S. L. S., Kowalik, J. S., and Pizzo, J. T., *Iterative Methods for Non-Linear Optimization Problems,* Prentice-Hall, Englewood Cliffs, NJ, 1972.

[10]Kahn, M. E. and Roth, B., "The Near-Minimum Time Control of Open-loop Articulated Kinematic Chains," *ASME Journal of Dynamic Systems, Measurement, and Control,* Vol. 93, Sept. 1971, pp. 164–172.

[11]Luh, J. Y. S., "An Anatomy of Industrial Robots and Their Controls," *IEEE Transactions on Automatic Control,* Vol. AC-28, Feb. 1983, pp. 133–153.

[12]Meier, E., *An Efficient Algorithm for Bang-Bang Control Systems Applied to a Two-Link Manipulator,* Ph.D. Dissertation, Department of Mechanical Engineering, Stanford Univ., Stanford, CA, Dec. 1986.

[13]Niv, M., and Auslander, D. M., "Optimal Control of a Robot with Obstacles," *Proceedings of the American Control Conference,* 1984, pp. 280–287.

[14]Pontryagin, L. S., Boltyanskii, V. G., Gamkrelidze, R. V., and Mishchenko, E. F., *The Mathematical Theory of Optimal Processes,* Wiley, New York, 1962.

[15]Prinz, M., *Optimal Control of Robot Manipulators,* Ph.D. Dissertation, Department of Mechanical Engineering, Stanford Univ., Stanford, CA, June 1986.

[16]Rajan, V. T., "Minimum Time Trajectory Planning," *IEEE International Conference on Robotics and Automation,* St. Louis, MO, March 1985, pp. 759–764.

[17]Sahar, G., and Hollerbach, J. M., "Planning of Minimum-Time Trajectories for Robot Arms," *Proceedings of the Conference on Robotics of the IEEE,* St. Louis, MO, March 1985.

[18]Scheinman, V., and Roth, B., "On the Optimal Selection and Placement of Manipulators," *Fifth CISM-IFToMM Symposium on Theory and Practice of Robots and Manipulators,* Udine, Italy, June 1984, pp. 25–32.

[19]Shin, K. G., and McKay, N. D., "Minimum-Time Control of Robotic Manipulators with Geometric Constraints," *IEEE Transactions on Automatic Control,* Vol. AC-30, June 1985, pp. 531–541.

[20]Sontag, E. E. and Sussmann, H. J., "Remarks on the Time-Optimal Control of Two-Link Manipulators," *Proceedings of the IEEE Conference on Decision and Control,* Dec. 1985, pp. 1643–1652.

[21]Sontag, E. D., and Sussmann, H. J., "Time-Optimal Control of Manipulators," *IEEE International Conference on Robotics and Automation,* San Francisco, April 1986.

[22]Wampler, C. W., II, *Computer Methods in Manipulator Kinematics, Dynamics, and Control: A Comparative Study,* Ph.D. Dissertation, Department of Mechanical Engineering, Stanford Univ., Stanford, CA, Dec. 1984.

[23]Weinreb, A., *Optimal Control with Multiple Bounded Inputs,* Ph.D. Dissertation, Departments of Electrical Engineering and Aeronautics and Astronautics, Stanford Univ., Stanford, CA, SUDAAR No. 554, 1984.

[24]Weinreb, A., and Bryson, A. E., Jr., "Optimal Control of Systems with Hard Control Bounds," *IEEE Transactions on Automatic Control,* Vol. AC-30, Nov. 1985.